

# Raman spectroscopy as a tool for quality and sterility analysis for tissue engineering applications like cartilage transplants

Marieke Pudlas<sup>1,2</sup>, Steffen Koch<sup>1,2</sup>, Carsten Bolwien<sup>3</sup>, Heike Walles<sup>1</sup>

<sup>1</sup> Fraunhofer Institute for Interfacial Engineering and Biotechnology, Stuttgart - Germany

<sup>2</sup> University of Stuttgart, Medical Interfacial Engineering, Stuttgart - Germany

<sup>3</sup> Fraunhofer Institute for Physical Measurement Techniques, Freiburg - Germany

**ABSTRACT:** At present, the production of tissue engineered cartilage requires the concurrent production of two identical transplants. One transplant is used for destructive quality control and the second one is implanted into the patient. A non-invasive characterization of such tissue engineering samples would be a promising tool to achieve a production process of just one transplant that is both implanted and tested. Raman spectroscopy is a method that satisfies this requirement by analyzing cells without lysis, fixation or the use of any chemicals. This pure optical technique is based on inelastic scattering of laser photons by molecular vibrations of biopolymers. Characteristic peaks in Raman spectra of cells could be assigned to typical biochemical molecules present in biological samples. For the analysis of chondrocytes present in cartilage transplants, the determination of the cell vitality as well as the discrimination of another cell type have been studied by Raman spectroscopy. Another bottleneck in such biological processes under GMP conditions is sterility control, as most of the commonly used methods require long cultivation times. Raman spectroscopy provides a good alternative to conventional methods in terms of time saving. In this study, the potential of Raman spectroscopy as a quality and sterility control tool for tissue engineering applications was studied by analyzing and comparing the spectra of cell and bacteria cultures. (Int J Artif Organs 2010; 33: 228-37)

**KEY WORDS:** Raman spectroscopy, Tissue engineering, Quality control, Sterility control

## INTRODUCTION

Articular cartilage is a complex, highly organized connective tissue that permits smooth, frictionless movement of diarthrodial joints. It is comprised of a relatively small number of chondrocytes, the only cell type present in cartilage. These cells are embedded in an extracellular matrix, which is produced and maintained by the chondrocytes and consists primarily of type II collagen, proteoglycans and water (1-3). Although cartilage has the ability to maintain itself, this tissue is vulnerable to injuries and diseases as it lacks blood or lymphatic vessels (4). Due to this property, the usual inflammation process does not occur and injuries do not heal. Furthermore, traumatic cartilage injuries cannot

be compensated by differentiated chondrocytes due to their loss of proliferation (5).

In order to replace damaged or lost cartilage tissue, a transplantation of tissue-engineered cartilage is a promising technique to repair cartilage defects. One of the first cartilage substitutes was autologous chondrocyte transplantation (ACT), which was established and has been in clinical use since the late 1900s (6, 7). This procedure is based on the implantation of a cell suspension consisting of cultured autologous chondrocytes beneath a tightly sealed periosteal patch. This concept is based on three main steps: firstly, the isolation of chondrocytes from a small hyaline cartilage biopsy; secondly, the expansion of these cells in monolayer culture; and thirdly, the implantation into

the cartilage defect (8). As chondrocytes are released from their native cartilage environment, they tend to lose their chondrocyte-specific phenotype over the cultivation time (9–12). In order to avoid this dedifferentiation, the imitation of the native cartilage environment during cell cultivation was sought. The cultivation of chondrocytes in three-dimensional scaffolds was thus established (10, 11, 13).

In order to guarantee that cells have not dedifferentiated, died or degenerated during cultivation time, a quality control tool for tissue engineering transplants is mandatory. Principally, the quality control standards for cartilage transplants should contain information about cell viability, the grade of differentiation, cell morphology, secretion levels of essential matrix components, and the total cell number (14, 15). Conventional quality testing of those products is carried out by destructive methods like immunohistological, molecular biochemical or microscopy techniques. These analytical methods are either invasive, require cell fixation, staining, labeling, lysis or affect cells vitality adversely. Additionally, for most methods complex sample preparations are necessary. In the case of matrix-based transplants the parallel production process of two transplants is needed due to the invasive analysis properties. One transplant is needed to ensure the quality standards and the second one is implanted into the patient. Consequently, it is simply assumed that both transplants possess identical properties.

Laser-based Raman spectroscopy, thanks to its key advantage of being able to probe cells under *in vivo* conditions, could overcome most of the limitations of common analytical methods described above (16). This purely optical technique is marker-free and non-destructive and does not induce cell damages if suitable laser wavelength and powers are used (17, 18).

Raman spectroscopy is a spectroscopic technique based on the detection of vibrational energy levels of a molecule. Every molecule has a unique set of vibrational modes, resulting in a distinct pattern of possible energy levels that the molecule may occupy. Light is able to induce the transition between different vibrational states of a molecule by either absorption of a photon or by the Raman process. In the first case, the total photon energy has to equal the energy difference between vibrational states. By contrast, the Raman process uses only a part of the photon's energy to drive the transition; the remaining light energy is sent out as a photon with less energy and thus a longer wavelength. In absorption spectroscopy the typical energy differences occurring in molecular vibrations correspond to light in

the infrared portion of the spectrum. Infrared absorption spectroscopy faces several technical complications, such as the fact that the molecular absorption spectrum can be dominated by the absorption of water molecules, comparably weak light sources, and low sensitivity detectors in the infrared.

In contrast to absorption spectroscopy, Raman spectroscopy is able to transpose the usable spectral region into the visible part of the light spectrum by using only energy differences between input and output photons. In principle, every laser wavelength can be used to record vibrational spectra. One major drawback of Raman spectroscopy is the inherent, extremely small probability of the vibrational energy transition event. Consequently, much light is needed to interact with a sample in order to yield a small amount of Raman photons: typically the ratio is on the order of  $1:10^8$  or less. The efficiency of the spectroscopic setup is therefore very important. Nowadays, a typical setup comprises a laser as a strong light source and an optical setup that efficiently focuses the laser onto the sample and collects the emitted Raman light. In recent years advances in optical components have driven the development of compact Raman spectrometers, typically based on a Raman edge filter as the main component of the system.

For the application of Raman spectroscopy as an analytical method for biological systems, the easy sample preparations as well as short integration times of only a few minutes are advantageous. Beyond these considerations, Raman spectroscopy has the potential to be implemented as an automatable method. Thus it is a promising tool for quality control applications, for which accurate and reliable measurements are mandatory.

As the vibrational energy levels a molecule may occupy are strongly coupled to the molecule's geometry, mass, charge, and bonds, each molecule's pattern is unique. Accordingly, its vibrational spectrum measured with infrared or Raman spectroscopy is unique. For a long time these techniques have been used in basic chemistry applications to identify unknown substances or for product quality control. However, more recently the application of the technique has been extended to the identification of complex mixtures of substances. The technique has been successfully implemented for detection of single cells and microorganisms and it has already been tested for some special biological applications (19, 20). Determinations of biochemical changes during cell cycle phases and those associated with tumorigenic transformations have been

made (21, 22). Different stages of cell vitality could be determined by Raman spectroscopy as well (23). The interaction of biomaterials and cells could be detected by Raman spectroscopy as spectra could be taken from the produced extracellular matrix which covers the scaffold (24). Additionally, a few studies have been carried out to prove the potential of Raman spectroscopy for tissue engineering applications. Notingher et al (2004) showed that the *in situ* identification of phenotypic differences in living cells, which are commonly used in bone tissue engineering, is possible (25). A comparison of Raman spectroscopy and other optical methods concerning the non-invasive analysis of engineered tissues was studied (26). It was shown that Raman spectroscopy reveals morphological and biochemical/ molecular and/or structural information of biological samples by spectroscopic analysis.

Determination of microbial contaminations is a further crucial task in the production process of tissue engineering products. Commercially available systems for the detection of contaminations are mostly based on physiological and nutritional characteristics of microorganisms (19). Depending on the type of microorganism, the identification process takes at least one day, but generally up to weeks (19, 27). The production of transplants, such as autologous chondrocyte transplants, takes place under clean room conditions, in order to guarantee the product sterility. The required sterility controls are done as intake, in-process, and final testing from supernatants of the biopsies, the cell culture, and the transplant. The results of these tests, especially of the final testing, may be too late, so that the transplant is implanted even before the final results of these tests have been obtained. Many analysis methods have been applied to address the requirements for a fast, sensitive, and reproducible technique for sterility testing and identification purposes. Some of these methods are PCR, mass spectroscopy, flow cytometry, and fluorescence spectroscopy (27-29). Other approaches deal with the use of vibrational spectroscopic techniques, mainly Raman spectroscopy and IR-spectroscopy. Several groups have reported the use of Raman spectroscopy in bacterial classification up to the strain level (19, 27, 30). However, nearly all of the groups use dried bacterial samples or single cells for the classification. Our approach deals with the usage of single bacteria analysis in a fluid environment for sterility testing and species identification. One aim of our work is to show that Raman spectroscopy can be used for sterility testing on a single cell level and in tissue engineering rel-

evant fluid samples to make the sterility testing even faster. The use of Raman spectroscopy as a quality control tool for tissue engineering products was investigated as well. The cell vitality of primary chondrocytes as well as the differentiation of two primary cell types were thus studied.

## MATERIAL AND METHODS

### *Cell isolation and culture*

Primary chondrocytes were isolated from 6-month-old porcine articular cartilage. Cartilage slices were taken from the macroscopically normal part of knee joints. The hyaline cartilage was cut into small pieces and enzymatically digested with type II collagenase (Serva Electrophoresis GmbH, Heidelberg, Germany). This isolation step was performed overnight at 37°C in a flask containing medium with 0.3 U/mL type II collagenase and a magnetic stir bar in order to separate the extracellular matrix completely from the chondrocytes. The resulting cell suspension was harvested by filtering, centrifugation and washing steps. The obtained cells were resuspended in culture medium and cell number and vitality were determined by cell counts using a hemocytometer and trypan blue vital dye. Dulbecco's modified Eagle's medium (DMEM)/ Hams F12 (PAA Laboratories GmbH, Pasching, Austria) containing 10% fetal calf serum (Gibco, Carlsbad, USA), 50 µg/mL ascorbic acid 2-phosphate (Sigma-Aldrich, Steinheim, Germany), and 1% Penicillin-Streptomycin (100x, Invitrogen, Carlsbad, USA) was used for isolation and cultivation. Chondrocyte cultivation was carried out in 75 cm<sup>2</sup> and 175 cm<sup>2</sup> cell culture flasks with 1,2\*10<sup>4</sup> cells/cm<sup>2</sup> in a humidified incubator at 37°C and 5% CO<sub>2</sub>.

Porcine stem cells were isolated from the bone marrow, which was extracted from the femoral shaft of 6-month-old animals and then stirred by a magnetic stir bar in 200 mL PBS<sup>+</sup> (PBS containing Mg<sup>2+</sup> and Ca<sup>2+</sup>) for 40 minutes in a flask at 37°C. Afterwards this suspension was filtered and centrifuged at 200 g for 10 minutes. Cells were washed with PBS<sup>+</sup> and centrifuged again for 10 minutes at 200 g. After additional resuspension with PBS<sup>+</sup> this cell suspension was layered upon a Ficoll gradient and centrifuged at room temperature for 30 minutes at 250 g. The interface buffy cell layer was collected, washed in PBS<sup>+</sup> and centrifuged again for 10 minutes at 200 g. This washing step

was repeated once. Afterwards cells were resuspended in culture medium as described above. Cell number and vitality were determined by cell counts using a hemocytometer and trypan blue vital dye. Stem cell cultivation was carried out in 75 cm<sup>2</sup> and 175 cm<sup>2</sup> cell culture flasks with  $6,7 \cdot 10^5$  cells/cm<sup>2</sup> in a humidified incubator at 37°C and 5% CO<sub>2</sub>. The culture medium was changed every 3 to 4 days.

### *Necrosis induction and detection*

Necrosis of primary chondrocytes was induced by incubating cells detached and resuspended in culture medium at 55°C in a preheated water bath for 90 minutes. Successful necrosis induction was proofed by a propidium iodid (PI) staining (Invitrogen, Carlsbad, USA). For this detection, the cell suspension of  $2\text{--}3 \cdot 10^6$  cells/mL was first washed twice with PBS<sup>+</sup> and then 100 µL of this cell suspension was incubated with 10 µL PI at room temperature for 15 minutes. Stained cells were used for Raman spectroscopy measurements.

### *Culture of microorganisms*

The microorganisms *B. subtilis* (DSMZ 347) and *E. coli* (DSMZ 498) were supplied by the German Collection of Microorganisms and Cell Cultures (DSMZ). The cultivation was carried out for 2 hours in medium consisting of 5 g/L peptone and 3 g/L meat extract at pH7. Spores from *B. subtilis* were obtained by cultivating *B. subtilis* on agar plates (15 g/L agar and 10 mg/L MnSO<sub>4</sub> x H<sub>2</sub>O) for 14 days. After cultivation spores were purified with Ultrasonic for 20 minutes at 60°C.

### *Raman spectroscopy*

The 785 nm Raman laser (Toptica Photonics AG, Munich, Germany) beam is coupled into a microscope (Olympus IX71), and the microscope objective focuses the laser onto the sample. In backscattering geometry the stray light is collected by the same objective and traverses the same light path, eventually reaching the Raman edge filter. The Stokes-shifted Raman light passes through this filter and is focused onto the entrance slit of the commercially available spectrograph (Kaiser Optical Systems Inc., Ann Arbor, MI, USA). An NIR-optimized, cooled CCD camera (Andor iDus, Belfast, Northern Ireland) is attached to the output port and used for data acquisition. The holographic grating of the spec-

trograph was chosen to provide the low-frequency region of the Raman spectrum from approximately 0 to 2000 cm<sup>-1</sup> with a spectral resolution of approximately 4 cm<sup>-1</sup>.

For Raman spectroscopy measurements, cells were trypsinized, resuspended in medium, and put into the measuring vessel, a glass bottom dish. From 25 to 30 cells were measured per experimental approach. Each Raman spectrum measured in a single location of a cell or bacterium was collected for 100 seconds. During Raman measurements cells and microorganisms were kept in cultivation medium to prevent cell collapse. In the case of measurements concerning the vitality status of cells, the necrotic status was confirmed by a positive PI staining determined in the fluorescence microscopy. Pure microorganism cultures as well as pure and sterile cell cultures were used for all investigations.

### *Data processing*

Data acquisition was performed with the software package Andor Solis provided by the camera manufacturer. Data processing including background subtraction and baseline correction was carried out with Opus® (Ver. 4.2, Bruker, Billerica, MA, USA). Further processing steps like smoothing and normalization as well as the principal component analysis (PCA) was done with the Unscrambler® (Ver. 9.7, Camo Software AS, Oslo, Norway).

### *Data analysis – Principal component analysis*

Each spectrum consists of many data points, but only a few of them contain useful information for cell analysis. The goal of the principal component analysis is to define a new dimensional space in which the largest variances in the Raman spectra are captured. These variances are represented by only a few principal components (PC) which identify the most important differences of the Raman spectra; PCA reduces the complex Raman spectral data to a few number of PCs. In most cases, the first 2 PCs account for more than 50% of the variances. This analysis was performed primarily on individual rather than averaged Raman spectra.

## RESULTS

The quality control of cells plays an important role in the production process of tissue engineered products. It is

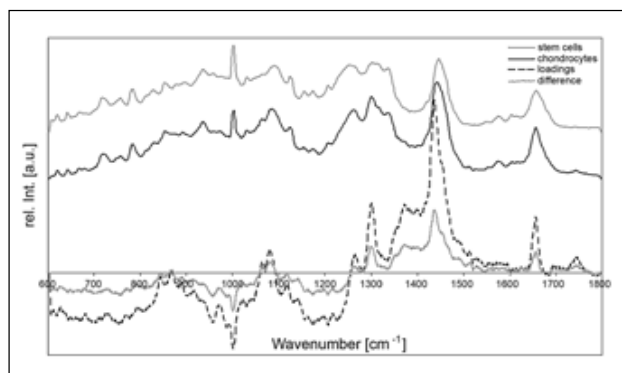


**Fig. 1** - Mean Raman spectra of primary chondrocytes and primary mesenchymal stem cells in the fingerprint range from 600  $\text{cm}^{-1}$  to 1800  $\text{cm}^{-1}$ . Also shown is the difference spectrum, obtained by subtracting the spectrum of the mesenchymal stem cells from the spectrum of primary chondrocytes. Loading values are plotted for the first principal component defined by the PCA plot in Figure 2. The higher the loadings value the greater the contribution to the PCA. The Raman spectra are shifted along the intensity axis for clarity.

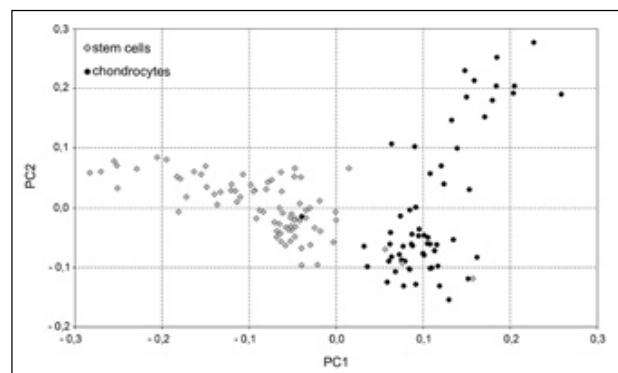


**Fig. 2** - Principal component analysis (PCA) plot comparing primary chondrocytes and primary mesenchymal stem cells. This result is based on the first and second principal component and shows two groups, which separate these two primary cell types. PC1 and PC2 account for 77% of the variance between the Raman spectra obtained from these cell types.

necessary to characterize cells before reimplantation into the patient by checking the cell viability and the grade of differentiation or secretion levels of essential matrix components, for example. This study focuses on the discrimination of primary cell types and the determination of the vitality status of cells by Raman spectroscopy. This technique allows a non-invasive, marker-free and rapid cell analysis and is a good alternative to common cell characterization methods. Furthermore, the discrimination of cells and microorganisms was studied by Raman spectroscopy as it is an important requirement for the sterility control of tissue engineered products.

The mean Raman spectra of primary chondrocytes and mesenchymal stem cells are shown in Figure 1. Also shown in this figure are the mean difference spectrum and loading values in order to identify the most significant spectral differences. In general, the higher the intensity of the loading spectrum, the higher is the variation in the spectra and the greater is the contribution to the PCA. The spectra of the studied cell types have almost the same structure, obtaining typical peaks of biomolecules like proteins, nucleic acids, lipids and carbohydrates. A peak assignment to biochemical molecules was previously carried out by several authors (20, 31-33). They found out that nucleic acids are characterized by peaks belonging to nucleotide and sugar-phosphate backbone vibrations. The Amide I and Amide III vibrations as well as the phenylalanine peak (1003  $\text{cm}^{-1}$ )

could be assigned to proteins. Lipid structures can be identified by bands at 1300  $\text{cm}^{-1}$ , 1437  $\text{cm}^{-1}$  as well as at 1660  $\text{cm}^{-1}$ , which mainly correspond to CH vibrations and C=C stretching of the aliphatic rest. However, there occur a few spectral differences for stem cells and chondrocytes, which are indicated in the similar structured difference and loading spectrum. These spectra show distinctive peaks in the regions of 1003  $\text{cm}^{-1}$ , 1300  $\text{cm}^{-1}$ , between 1400  $\text{cm}^{-1}$  and 1500  $\text{cm}^{-1}$  and between 1600  $\text{cm}^{-1}$  and 1700  $\text{cm}^{-1}$ . Most of these peaks are due to differences in the Raman signal intensities, but some are caused by spectral differences in the obtained spectra.

The identification of spectral differences in a data set of several Raman spectra was carried out by a sensitive statistical method. Principal Component Analysis (PCA) extracts the most important information of the Raman spectra. As one result of the PCA, the principal components (PC) are plotted against each other. Each obtained score (dot) in a PCA plot represents a spectrum of one cell. The lowest PCs contain the most useful information while the remaining ones contain noise.

In Figure 2, a PCA plot of spectra obtained from chondrocytes and mesenchymal stem cells is demonstrated. This plot shows two distinct groups, each containing the scores of one cell type. For this data transformation, only the first two principal components are necessary as they explain 77% of the variances between the spectra. The

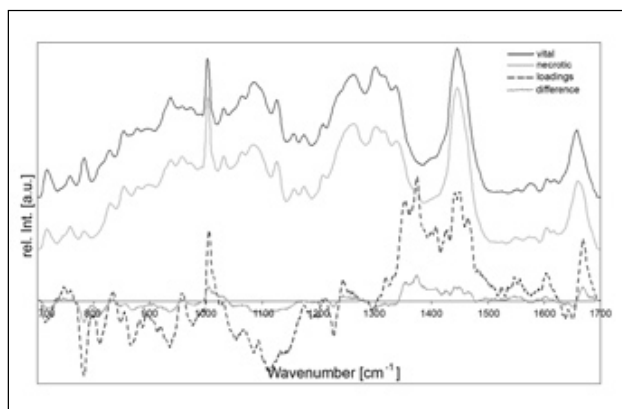


**Fig. 3** - Mean Raman spectra of vital and necrotic chondrocytes in the fingerprint range from 700  $\text{cm}^{-1}$  to 1700  $\text{cm}^{-1}$ . Also shown is the difference spectrum, obtained by subtracting the spectrum of the vital cells from the spectrum of necrotic cells. Loading values are plotted for the first principal component defined by the PCA plot in Figure 4. The Raman spectra are shifted along the intensity axis for clarity.

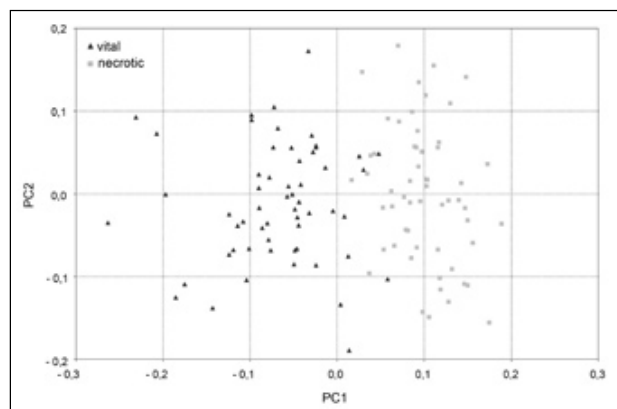


**Fig. 4** - Plot displays the results of the principal component analysis (PCA) using the first and second principal components for spectra taken from vital and necrotic chondrocytes. It shows two distinct groups. PC1 and PC2 account for 64% of the variance between the Raman spectra obtained from these cells with different vitality statuses.

separation occurs along the PC1 direction. Further investigations have been made to estimate biochemical changes due to necrosis of chondrocytes by Raman spectroscopy. The averaged Raman spectra obtained from necrotic and vital cells are plotted in Figure 3. The loading spectrum, which is significantly structured, and the less-structured difference spectrum are demonstrated as well. The results of the PCA performed on Raman spectra of vital and necrotic cells are shown in Figure 4. The plot of the first PC versus the second PC shows the distinction between the two vitality statuses along the PC1 axis, accounting for 64% of this variance.

Besides the characterization of cells for quality control issues, the control of sterility is an essential task in tissue engineering procedures. For these controls it is not necessary to detect microorganisms on the strain level, but to detect every potential microbiological contamination. It is thus necessary to discriminate between cells and bacteria on a single cell level based on its Raman spectrum. In Figure 5 the average spectra of chondrocytes, *E. coli*, *B. subtilis* and the spores of *B. subtilis* are shown. Noticeable characteristic peaks can be seen in the spectrum of the bacterial spores at the positions of 661, 822, 1017, 1395 and 1575  $\text{cm}^{-1}$ . These bands correspond to different vibrational modes of Calcium-Dipicolinate (CaDPA), one of the main components of bacterial spores (34). The spectra of the two bacteria, *E. coli* and *B. subtilis* look quite similar.

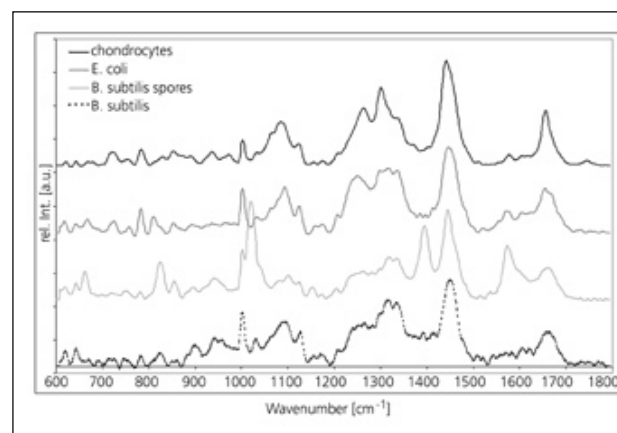


**Fig. 5** - Average Raman spectra of primary chondrocytes, *E. coli*, *B. subtilis* spores and *B. subtilis* (from top) in the fingerprint range from 600  $\text{cm}^{-1}$  to 1800  $\text{cm}^{-1}$ . The Raman spectra are shifted along the intensity axis for clarity.

The spectrum of the chondrocytes shows only small differences compared to the spectra of bacteria, mainly in the Amid III band at 1255  $\text{cm}^{-1}$  and the Amid I band at 1656  $\text{cm}^{-1}$ . The PCA in Figure 6 shows clear differences between the bacterial spores and the bacteria and chondrocytes according to the differences visible in Figure 5. The PCA for most of the measurements shows a clear clustering along PC 1 and PC 3. The loadings for the PCA shown

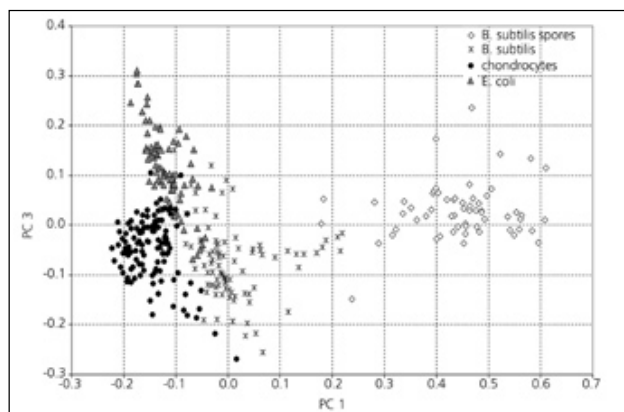


**Fig. 6** - Principal component analysis plot comparing primary chondrocytes, *E. coli*, *B. subtilis* and spores of *B. subtilis*. This result is based on the first and third principal component, which describe 57% of the total variance.

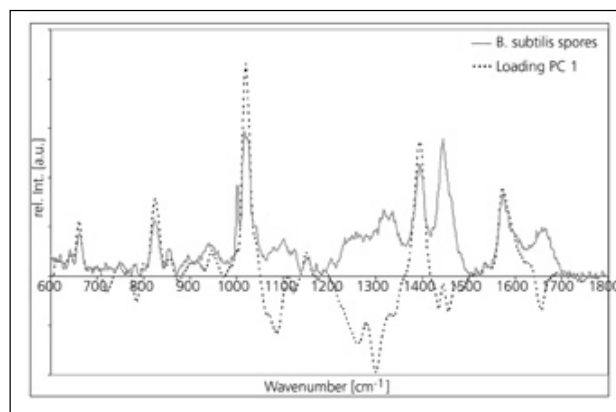


**Fig. 7** - Loadings of the first PC according to the PCA shown in Figure 6. The loadings are similarly structured to the spectrum of the *B. subtilis* spores. The negative values correspond mainly to protein bands around 1300  $\text{cm}^{-1}$  (Amide III), 1656  $\text{cm}^{-1}$  (Amide I) and the area around 1090  $\text{cm}^{-1}$  (not assigned).

in Figure 6 are displayed in Figure 7 and Figure 8. For PC 1 there is a clear positive correlation between the original spore spectrum and the loading spectrum. The differences between the bacteria and chondrocytes are smaller, resulting in broader areas in the loading spectrum for the discrimination.

## DISCUSSION

In the field of cartilage tissue engineering it is preferable to develop marker-free and non-destructive analysis methods for tissues and cells in order to achieve a safe, economic production and quality control process. As a non-contact laser based technique, Raman spectroscopy has the potential to fulfill these requirements.

The first investigations that were performed were to characterize chondrocytes. For this purpose, the separation of chondrocytes from another cell type by Raman spectroscopy was targeted. In our study we used mesenchymal stem cells, as this cell type is also a candidate for the repair of articular cartilage defects (35). Furthermore, cell clones with stem-cell properties were identified in articular cartilage, which makes a separation of these two cell types useful (36). In order to make sure that chondrocytes survived the isolation step as well as the cultivation time *ex vivo* the vitality status needs to be proven before

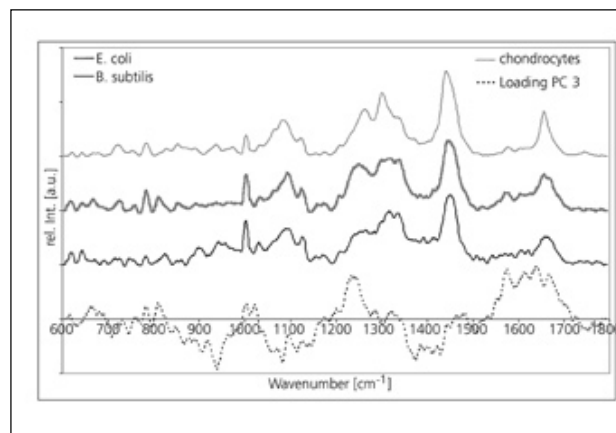


**Fig. 8** - Averaged Raman spectra of *E. coli*, *B. Subtilis* and primary chondrocytes are displayed. Loading values are plotted for the third PC defined by the PCA plot in Figure 6. The Raman spectra are shifted along the intensity axis for clarity.

implantation. In the first step we studied necrotic and vital chondrocytes by Raman spectroscopy.

Although the PCA of spectra obtained from cells is able to discriminate between cell types and between different vitality statuses, the biochemical variations on which the discrimination is based on needs to be studied in more detail. For this purpose, the significant Raman peaks that are responsible for the discriminations of different cellular

groups can be extracted by analyzing the loading spectra. In order to ascertain which cell type or vitality status a peak of the loadings spectrum has a higher influence on, the algebraic sign of the loadings and the score values have to be multiplied. A positive value for the studied peak corresponds to a higher concentration of the associated biochemical substance for the analyzed cell type.

The most intensive bands in the loading spectrum, which results from the comparison of chondrocytes and mesenchymal stem cells (Fig. 1) are present at 1300  $\text{cm}^{-1}$ , 1437  $\text{cm}^{-1}$  and 1657  $\text{cm}^{-1}$ . These peaks are assigned to lipid structures (32). They result from the spectra of chondrocytes and could be explained by the typical lipid inclusions in chondrocytes, which are built up as a reservoir due to their slow metabolism (37). A further peak appears at 1003  $\text{cm}^{-1}$ , which is assigned to phenylalanine and is present in almost every Raman spectra obtained from biological samples. The intensity of the phenylalanine peak gives evidence about the protein concentration in cells (18). Apparently, the protein concentration is higher in stem cells than in chondrocytes, which could be explained by the higher metabolic activity of stem cells in contrast to cells present in articular cartilage.

Due to the heat-induced necrosis of chondrocytes, a change of the cellular protein structure was expected. These assumptions have been confirmed by the structural shifts in the Raman spectra of necrotic and vital cells. Especially the peak at 1003  $\text{cm}^{-1}$ , which corresponds to the ring stretching of phenylalanine, is a good necrosis marker as it is increased in the spectra of dead cells. Kunapareddy et al (2008) additionally observed an increase of the protein concentration in necrotic cells, although they did not detect a change in the phenylalanine peak (38). Another significant difference between vital and necrotic cells lies in the spectral region at 788  $\text{cm}^{-1}$ , which is assigned to the phosphate backbone of the DNA (18, 39). The breakdown of the phosphodiester bonds in dead cells are indicated by the reduction of this peak. A further spectral difference associated with changes in the DNA structure is present at a wavelength of 937  $\text{cm}^{-1}$ , which is reduced in necrotic cells. This peak is assigned to molecular vibrations of the  $\alpha$  helix backbone (25). These changes could be attributed to the heat-induced denaturations of proteins and DNA in such cells. The band at 1373  $\text{cm}^{-1}$  is assigned to DNA bases (20, 32, 33). It is just present in the spectrum of necrotic cells and could also be used as an indication for the death of cells. Further suitable markers for necrosis like the lipid

peak at 1660  $\text{cm}^{-1}$  have been identified earlier by the investigation of vital and dead cells from the cell line A549 (39). These results could be confirmed for the studied primary chondrocytes and indicate an increase in the lipid concentration in necrotic cells.

Identification of microorganisms based on Raman spectroscopy is not a new approach. There are several groups which showed that Raman spectroscopy is a powerful tool for this purpose (19, 27, 28). However, this work deals with the possibility of detecting single cells in a fluid environment, detecting chemical differences between cells and bacteria, and giving a starting point for the detection of the biological variation within one type of cell, which is an important point for the identification of microorganisms and cells. The results show that there are clear differences between *Bacillus subtilis* spores, bacteria and chondrocytes. These differences are already visible in the spectral regions around 661, 822, 1017, 1395 and 1575  $\text{cm}^{-1}$  which correspond to the results of earlier studies (34). The PCA is calculated for PC1 mainly on these spectral differences as it is visible in the loadings for PC1. Nevertheless, the differentiation of cells and bacteria based on Raman spectroscopy is more complicated. The PCA demonstrated in Figure 6 shows that there are some detectable differences between cells and bacteria. The main differences can be found in the protein concentrations and differences in the proteins detected, represented by the amid vibrations at 1255 and 1656  $\text{cm}^{-1}$ . A further significant band in the loading spectrum is present at 937  $\text{cm}^{-1}$  and could be assigned to DNA. Other differences for the discrimination are not assignable to chemical compounds in the cells, but the PCA clearly shows that there are systematic differences within the spectral data of the different cell types. The spectral areas will be main topics of further investigations.

This study conclusively proved the feasibility of separating different phenotypes of cells by a multivariate analysis of their Raman spectra for use of this technique as a quality control tool in tissue engineering processes. The detection of biochemical differences, which are present between chondrocytes and stem cells and cell vitality statuses of chondrocytes, respectively, could be identified by their corresponding Raman spectra. Moreover, preliminary studies of our group show good results for the determination of the differentiation status of chondrocytes by Raman spectroscopy, by detecting the absence of type II collagen and aggrecan and the presence of type I collagen. These results, obtained from just one measurement, contain some



of the information needed for the determination of the quality of chondrocytes used in tissue engineering applications. From this it follows that Raman spectroscopy is a promising method for the rapid, non-invasive and marker-free characterization of tissue engineered products like cartilage transplants. As the separation of cells, bacteria and spores by their Raman spectra is possible in fluid samples, this technique seems to be a good alternative for routine, long-lasting sterility control methods. Investigations concerning contaminated cell cultures need to be conducted in the future in order to validate this technique. Further studies need to be carried out concerning the characterization of cells embedded in a matrix in order to apply Raman spectroscopy as a fully automated and non-destructive method in the field of matrix-based tissue engineering transplants. For the automatable measurement of potential contami-

nations, particles present in the supernatant need to be positioned by filtering through a suitable membrane. The optical recognition of particles like bacteria, cells or cell debris is followed by the measurement procedure.

**Financial support:** Fraunhofer Society, 80007 Munich, Germany.

**Conflict of interest statement:** None.

**Meeting presentation:** ESAO conference 2009, Compiègne, France, September 3, 2009; World Conference of Regenerative Medicine, 2009, Leipzig, Germany, October 29, 2009.

Address for correspondence:

Marieke Pudlas  
Fraunhofer Institute for Interfacial Engineering and Biotechnology  
Nobelstr. 12  
70569 Stuttgart, Germany  
e-mail address: marieke.pudlas@igb.fraunhofer.de

---

## REFERENCES

1. Mayne R. Cartilage collagens. What is their function, and are they involved in articular disease? *Arthritis Rheum* 1989; 32: 241-46.
2. Miller EJ. Biochemical characteristics and biological significance of the genetically-distinct collagens. *Mol Cell Biochem* 1976; 13: 165-92.
3. Kuettner KE. Biochemistry of articular cartilage in health and disease. *Clin Biochem* 1992; 25: 155-63.
4. Mankin HJ. The response of articular cartilage to mechanical injury. *J Bone Joint Surg (Am)* 1982; 64: 460-6.
5. Schulze-Tanzil G. Activation and dedifferentiation of chondrocytes: implications in cartilage injury and repair. *Ann Anat* 2009; 191: 325-38.
6. Grande DA, Pitman MI, Peterson L, Menche D, Klein M. The repair of experimentally produced defects in rabbit articular cartilage by autologous chondrocyte transplantation. *J Orthop Res* 1989; 7: 208-18.
7. Brittberg M, Lindahl A, Nilsson A, Ohlsson C, Isaksson O, Peterson L. Treatment of deep cartilage defects in the knee with autologous chondrocyte transplantation. *N Engl J Med* 1994; 331: 889-95.
8. Marlovits S, Zeller P, Singer P, Resinger C, Vécsei V. Cartilage repair: generations of autologous chondrocyte transplantation. *Eur J Radiol* 2006; 57: 24-31.
9. Zlabinger GJ, Menzel JE, Steffen C. Change in collagen synthesis of human chondrocyte culture. I. Development of a human model, demonstration of collagen type conversion by immunofluorescence. *Rheumatol Int* 1986; 6: 63-8.
10. Benay PD, Shaffer JD. Dedifferentiated chondrocytes reexpress the differentiated collagen phenotype when cultured in agarose gels. *Cell* 1982; 30: 215-24.
11. Domm C, Schünke M, Christesen K, Kurz B. Redifferentiation of dedifferentiated bovine articular chondrocytes in alginate culture under low oxygen tension. *Osteoarthritis Cartil* 2002; 10: 13-22.
12. Schulze-Tanzil G, de Souza P, Villegas Castrejon H, et al. Redifferentiation of dedifferentiated human chondrocytes in high-density cultures. *Cell Tissue Res* 2002; 308: 371-9.
13. Bonaventure J, Kadhon N, Cohen-Solal L, et al. Reexpression of cartilage-specific genes by dedifferentiated human articular chondrocytes cultured in alginate beads. *Exp Cell Res* 1994; 212: 97-104.
14. Schneider U, Breusch SJ, von der Mark K. Aktueller Stellenwert der autologen Chondrozytentransplantation. [Current status of autogenous chondrocyte transplantation]. [article in German]. *Z Orthop* 1999; 137: 386-2.
15. Fritsch KG, Josimovic-Alasevic O. Chondroneogenese durch autologe Chondrozytentransplantation (ACT). [Chondroneogenesis by autologous chondrocyte transplantation (ACT): a cell biological view of consequences for diagnosis and therapy]. [article in German]. *Arthroskopie* 1999; 12: 43-9.
16. Puppels GJ, de Mul FF, Otto C, Greve J, Robert-Nicoud M, Arndt-Jovin DJ, Jovin TM. Studying single living cells and chromosomes by confocal Raman microspectroscopy. *Nature* 1990; 347: 301-3.
17. Puppels GJ, Olminkhof JH, Segers-Nolten GM, Otto C, de

- Mul FF, Greve J. Laser irradiation and Raman spectroscopy of single living cells and chromosomes: sample degradation occurs with 514.5 nm but not with 660 nm laser light. *Exp Cell Res* 1991; 195: 361-7.
18. Notingher I, Verrier S, Romanska H, Bishop AE, Polak JM, Hench LL. In situ characterisation of living cells by Raman spectroscopy. *Spectrosc* 2002; 16: 43-51.
19. Maquelin K, Kirschner C, Choo-Smith LP, et al. Prospective study of the performance of vibrational spectroscopies for rapid identification of bacterial and fungal pathogens recovered from blood cultures. *J Clin Microbiol* 2003; 41: 324-9.
20. Notingher I, Hench LL. Raman microspectroscopy: a noninvasive tool for studies of individual living cells in vitro. *Expert Rev Med Devices* 2006; 3: 215-34.
21. Swain RJ, Jell G, Stevens MM. Non-invasive analysis of cell cycle dynamics in single living cells with Raman microspectroscopy. *J Cell Biochem* 2008; 104: 1427-38.
22. Yu C, Gestl E, Eckert K, Allara D, Irudayaraj J. Characterization of human breast epithelial cells by confocal Raman microspectroscopy. *Cancer Detect Prev* 2006; 30: 515-22.
23. Notingher I, Verrier S, Haque S, Polak JM, Hench LL. Spectroscopic study of human lung epithelial cells (A549) in culture: living cells versus dead cells. *Biopolymers* 2003; 72: 230-4.
24. Jones JR, Vats A, Notingher I, Gough JE, Tolley NS, Polak JM, Hench LL. In Situ Monitoring of Chondrocyte Response to Bioactive Scaffolds Using Raman Spectroscopy. *Key Eng Mater* 2005; 284-286: 623-626.
25. Notingher I, Jell G, Lohbauer U, Salih V, Hench LL. In situ non-invasive spectral discrimination between bone cell phenotypes used in tissue engineering. *J Cell Biochem* 2004; 92: 1180-92.
26. Georgakoudi I, Rice WL, Hronik-Tupaj M, Kaplan DL. Optical spectroscopy and imaging for the noninvasive evaluation of engineered tissues. *Tissue Eng Part B Rev* 2008; 14: 321-40.
27. Rösch P, Harz M, Schmitt M, Peschke KD, et al. Chemotaxonomic identification of single bacteria by micro-Raman spectroscopy: application to clean-room-relevant biological contaminations. *Appl Environ Microbiol* 2005; 71: 1626-37.
28. Ivnitski D, Abdel-Hamid I, Atanasov P, Wilkins E. Biosensors for detection of pathogenic bacteria. *Biosens Bioelectron* 1999; 14: 599-624.
29. Al-Khaldi SF, Mossoba MM. Gene and bacterial identification using high-throughput technologies: genomics, proteomics, and phonemics. *Nutrition* 2004; 20: 32-8.
30. Kirschner C, Maquelin K, Pina P, et al. Classification and identification of enterococci: a comparative phenotypic, genotypic, and vibrational spectroscopic study. *J Clin Microbiol* 2001; 39: 1763-70.
31. De Gelder J, De Gussem K, Vandenabeele P, Moens L. Reference database of Raman spectra of biological molecules. *J Raman Spectrosc* 2007; 38: 1133-47.
32. Krafft C, Knetschke T, Siegner A, Funk RHW, Salzer R. Mapping of single cells by near infrared Raman microspectroscopy. *Vib Spectrosc* 2003; 32: 75-83.
33. Chan JW, Taylor DS, Zwerdling T, Lane SM, Ihara K, Huser T. Micro-Raman spectroscopy detects individual neoplastic and normal hematopoietic cells. *Biophys J* 2006; 90: 648-56.
34. De Gelder J, Scheldeman P, Leus K, Heyndrickx M, Vandenabeele P, Moens L, De Vos P. Raman spectroscopic study of bacterial endospores. *Anal Bioanal Chem* 2007; 389: 2143-51.
35. Kafienah W, Mistry S, Dickinson SC, Sims TJ, Learmonth I, Hollander AP. Three-dimensional cartilage tissue engineering using adult stem cells from osteoarthritis patients. *Arthritis Rheum* 2007; 56: 177-87.
36. Barbero A, Ploegert S, Heberer M, Martin I. Plasticity of clonal populations of dedifferentiated adult human articular chondrocytes. *Arthritis Rheum* 2003; 48: 1315-25.
37. Moll KJ. Allgemeine Anatomie und Histologie. In: Anatomie. Munich: Urban & Fischer; 2006: 91-4.
38. Kunapareddy N, Freyer JP, Mourant JR. Raman spectroscopic characterization of necrotic cell death. *J Biomed Opt* 2008; 13: 054002.
39. Verrier S, Notingher I, Polak JM, Hench LL. In situ monitoring of cell death using Raman microspectroscopy. *Biopolymers* 2004; 74: 157-162.